

## HYDROTHERMAL GROWTH AND SQUEEGEE METHOD IN THE FABRICATION OF MIXED-PHASE TiO<sub>2</sub> NANOSTRUCTURES

Muqoyyanah<sup>1,2</sup>, Suriani Abu Bakar<sup>1,2\*</sup>, Azmi Mohamed<sup>1,3</sup>, Norhayati Hashim<sup>1,3</sup>, Mohamad Hafiz Mamat<sup>4</sup>, Mohd Firdaus Malek<sup>4,5</sup>, and Mohd Khairul Ahmad<sup>6</sup>  
\*e-mail: [absuriani@yahoo.com](mailto:absuriani@yahoo.com)

<sup>1</sup>*Nanotechnology Research Centre,*

<sup>2</sup>*Department of Physics,*

<sup>3</sup>*Department of Chemistry,*

*Faculty of Science and Mathematics, Universiti Pendidikan Sultan Idris,  
35900 Tanjung Malim, Perak, Malaysia.*

<sup>4</sup>*NANO-ElecTronic Centre (NET), Faculty of Electrical Engineering,*

<sup>5</sup>*NANO-SciTech Centre (NST), Institute of Science (IOS),*

*Universiti Teknologi MARA (UiTM), 40450 Shah Alam, Selangor, Malaysia.*

<sup>6</sup>*Microelectronic and Nanotechnology–Shamsuddin Research Centre (MiNT-SRC),  
Faculty of Electrical and Electronic Engineering, Universiti Tun Hussein Onn  
Malaysia, 86400 Parit Raja, Batu Pahat, Johor, Malaysia.*

### ABSTRACT

In this work, the modification of TiO<sub>2</sub> nanostructures based on its morphology and crystallinity phase were fabricated using a simple method. Hydrothermal growth method was used to synthesize nanorods and nanoflowers, while nanoparticles was applied using squeegee method. The average length and diameter of the as-grown nanorods were 3.5 and 46-215 nm, respectively. Meanwhile, the average total thickness and band gap value of mixed-phase TiO<sub>2</sub> nanostructures were 15.98-24.54 nm and 2.84 eV, respectively. Based on its structural and electrical properties, the fabricated film has great potential to be applied as photoanode semiconductor layer for dye-sensitized solar cells application.

Key words: TiO<sub>2</sub>, Nanostructures, Mixed-phase, Hydrothermal, Squeegee.

### ABSTRAK

Dalam penelitian ini, modifikasi struktur nano TiO<sub>2</sub> berdasarkan morfologi dan fase kristalinitasnya difabrikasi menggunakan metode sederhana. Metode pertumbuhan hidrotermal digunakan untuk mensintesis batang nano dan bunga nano, sementara untuk partikel nano diterapkan menggunakan metode squeegee. Rata-rata panjang dan diameter batang nano adalah masing-masing 3,5 dan 46-215 nm. Sementara itu, total rata-rata ketebalan dan nilai *band gap* dari fase campuran struktur nano TiO<sub>2</sub> adalah masing-masing 15,98-24,54 nm dan 2,84 eV. Berdasarkan sifat struktural dan listriknya, film yang dibuat memiliki potensi besar untuk diaplikasikan sebagai lapisan semikonduktor fotoanoda untuk aplikasi sel surya *dye-sensitized*.

Kata kunci: TiO<sub>2</sub>, struktur nano, fase campuran, hidrotermal, Squeegee.

## INTRODUCTION

Titanium dioxide ( $\text{TiO}_2$ ) becomes the most investigated metal oxides materials due to its wide range of applications and suitable for many experimental techniques (Diebold, 2003).  $\text{TiO}_2$  has several nanostructures, such as nanoparticle, nanorod, nanoflower, nanowire, nanotube, and hollow hemisphere. Meanwhile, anatase, rutile, and brookite are the crystallinity phase known for  $\text{TiO}_2$ . Each nanostructures and crystallinity phase have its own advantages and disadvantages. Brookite is known as metastable phase thus rarely used, while rutile is known as the most stable phase among other phases and has larger grain size as compared to anatase. The smaller grain size of anatase becomes an advantage due to the larger surface area as compared to rutile. Anatase also has the widest band gap ( $E_g$ ) among other phases which is useful in electronic applications [Lei, *et.al.*, 2016]. Based on those facts, the synthesis of mixed-phase  $\text{TiO}_2$  between rutile and anatase could yield a better electrical performance (Mehmood, *et.al.*, 2014). Some methods to synthesize  $\text{TiO}_2$  are pulsed laser deposition, hydrolysis method, hydrothermal growth, and solvothermal method.

Photocatalyst material, gas sensor, corrosion-protective coating, optical coating, Li-based batteries, and electrochromic devices are some of the applications which utilize  $\text{TiO}_2$ . In addition,  $\text{TiO}_2$  is also used in paint industries and cosmetic products as white pigment and even in medical as bone implant (Diebold, 2003). Among those applications,  $\text{TiO}_2$  as photocatalyst material gains a lot of interest since the invention of dye-

sensitized solar cells (DSSCs) in 1991 (O'Regan and Grätzel, 1991; Ahmad, *et.al.*, 2015; Zhang, *et.al.*, 2006; Lee, *et.al.*, 2014). Based on several investigations,  $\text{TiO}_2$  shows better performance as compared to ZnO and  $\text{SnO}_2$  which are usually used as photoanode semiconductor layer (Han, *et.al.*, 2009; Fukai, *et.al.*, 2007; Bauer, *et.al.*, 2002). Moreover, the properties of  $\text{TiO}_2$  which are chemically and physically stable, low-cost, good electronic properties, non-toxic, and large effective surface area are needed in dye adsorption process and suitable as well as become the advantages for DSSCs application (Lei, *et.al.*, 2016, Qin, *et.al.*, 2015; Tamilselvan, *et.al.*, 2012; Hwang, *et.al.*, 2012). The adsorption process becomes an important factor in DSSCs process which affect the DSSCs energy conversion efficiency ( $\eta$ ). The  $\eta$  value is affected by the amount of flowing electrons through the circuit indicated by short current density ( $J_{sc}$ ) value. The morphology and crystallinity phase of  $\text{TiO}_2$  absolutely affect the  $J_{sc}$  value thus their crystallinity need to be greatly considered in terms of structural optimization (Mehmood, *et.al.*, 2014; Zhu, *et.al.*, 2014; Gong, *et.al.*, 2012). Another important factor is the chosen substrate which should have high electrical conductivity and optically transparent. Sima *et al.* (Sima, *et.al.*, 2010) investigated the DSSCs performance by comparing indium-doped tin oxide and fluorine-doped tin oxide (FTO) as substrates. Based on the result, FTO shows a lower sheet resistance and thermally-stable thus it is recommended for DSSCs application.

In this work, we synthesize rutile TiO<sub>2</sub> nanorods—nanoflowers and mix them with anatase TiO<sub>2</sub> nanoparticles. Nanorods and nanoflowers were synthesized using hydrothermal growth (Ahmad, *et.al.*, 2015), while nanoparticles was synthesized using squeegee method (Zhang, *et.al.*, 2006).

## MATERIALS AND METHODS

FTO substrate was cut into 2×1 cm<sup>2</sup> dimension and cleaned using acetone, methanol, and deionize (DI) water for 15 minutes, respectively. The substrate was then placed on autoclave with the conductive surface facing upward. Hydrothermal solution for TiO<sub>2</sub> nanorods and nanoflowers growth were prepared based on previous study conducted by Ahmad, et al. [Ahmad, *et.al.*, 2015]. 120 ml of hydrochloric acid and 120 ml of DI water was stirred for 5 minutes until well-mixed before adding 6 ml of titanium butoxide dispersing drop by drop to the solution. Clear hydrothermal solution was obtained after stirring for another 10 minutes and directly poured into autoclave. Hydrothermal growth process was performed at 150°C for 5 hours. The grown films were then taken out from the autoclave after cooled down to room temperature followed by rinsing using DI water and drying in room temperature.

The second layer of the film was produced by applying TiO<sub>2</sub> paste based on simple squeegee method (Zhang, *et.al.*, 2006) on top of the as-grown TiO<sub>2</sub> nanorods and nanoflowers. 7.5 ml of ethanol was poured into 1.75 g titanium (IV) oxide and stirred until a paste formed followed by adding 0.25 ml of titanium (IV) isopropoxide and stirred until the prepared paste became

well-mixed with low agglomeration. The obtained paste was sonicated for 5 minutes in room temperature and rolled over the fabricated film's first layer using glass rod and heated in electric oven for 10 minutes at 150°C. The films was annealed at 450°C for 1 hour before processing with physical characterizations. Several characterization, such as field emission scanning electron microscopy (FESEM), micro-Raman spectroscopy, energy dispersive X-ray (EDX), and UV-Vis spectroscopy were used to investigate the morphology, lattice crystallinity, and electrical performance of the fabricated film.

## RESULTS AND DISCUSSIONS

FESEM images of the as-grown TiO<sub>2</sub> nanorods are presented in Fig. 1. Based on Fig. 1 (a), it can be shown that the synthesized nanorods was grown uniformly and densely. The crystal structure of nanorods was in tetragonal shape with diameters range of 46–215 nm as shown in Fig. 1 (b). Cross section image of fabricated film's first layer in Fig. 1 (c) reveals the perpendicular direction and high-density nanorods grown on FTO substrate. The results was in good agreement with Ahmad et al. (Ahmad, *et.al.*, 2015). Several size of nanoflowers which grow rarely in some spot of nanorods were also observed. The average length of nanorods was 3.5 nm, which was a bit longer compared to the previous result (Ahmad, *et.al.*, 2015). Anatase TiO<sub>2</sub> nanoparticles was also seen to be uniformly spread and completely covered nanorods as shown in Fig. 1 (d). The large surface area of nanoparticles due to the small grain size of particles gives an advantage if it

is applied as photoanode semiconductor layer which increase the dye adsorption. The study reveal that the maximum dye adsorption led to the increment of electron excitation thus improve the  $J_{SC}$  value. As a result of this, high  $\eta$  will be achieved. A closer view in Fig. 1 (e) shows a closely interconnected particles which is believed to give an advantage in electrons transfer to the nanorods. The shape and direction of as-grown

nanorods perpendicular to the substrate makes the electrons directly and easily move to FTO substrate. Fig. 1 (f) shows the cross section view of fabricated film thickness. Based on the image, the film thickness range from 15.98 to 24.54  $\mu\text{m}$ . EDX analysis as shown in Table 1 confirms titanium and oxygen as element compound of fabricated mixed-phase  $\text{TiO}_2$  nanostructures.

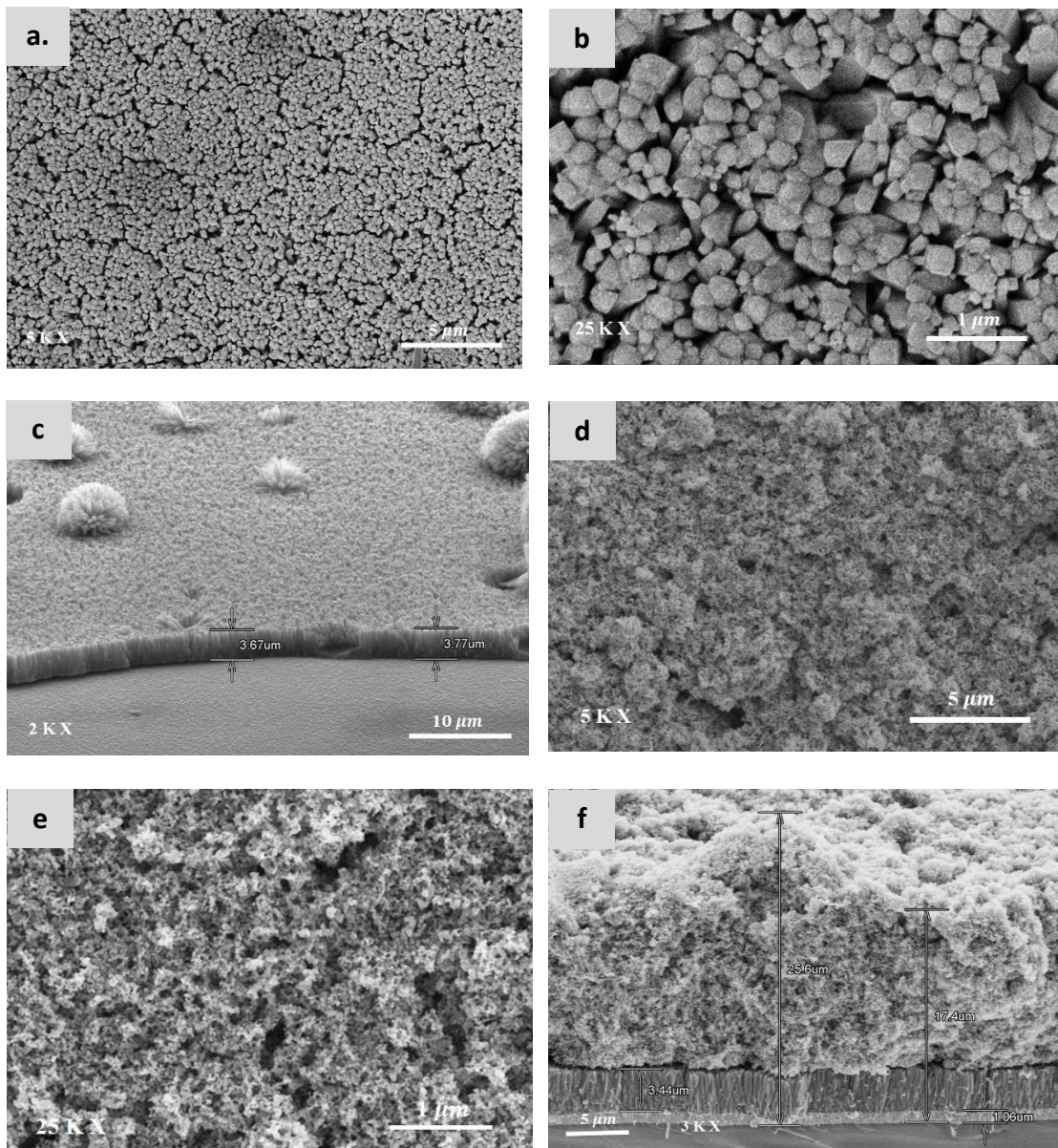


Fig. 1. FESEM images of fabricated mixed-phase TiO<sub>2</sub> nanostructures; (a)-(b) TiO<sub>2</sub> nanorods top view and (c) its cross section which contains nanoflowers, (d)-(e) TiO<sub>2</sub> nanoparticles top view and (f) fabricated film thickness cross section.

Table 1. EDX analysis of fabricated mixed-phase TiO<sub>2</sub> nanostructures.

Element compound	Weight (%)	Atomic (%)
Titanium (Ti)	56.05	29.87
Oxygen (O)	43.95	70.13

Fig. 2 shows micro-Raman spectra for both nanorods and mixed-phase of TiO<sub>2</sub> nanostructures films. Based on Fig. 2 (a), the synthesized TiO<sub>2</sub> nanorods was confirmed in rutile phase shown by four major peaks at 117, 237, 444, and 607 cm<sup>-1</sup>. Two prominent peaks at 444 and 607 cm<sup>-1</sup> shows a high intensity indicated that there were lots of nanorods compared to nanoflowers which confirm the analysis by FESEM. The micro-Raman spectra of mixed-phase TiO<sub>2</sub> did not shifted much after nanoparticles were

applied on top of the nanorods as shown in Fig. 2 (b). The additional peaks at 144 and 516 cm<sup>-1</sup> are known as anatase phase which confirmed that the synthesized film are in mixed-phase of rutile and anatase phase. The two prominent peaks of rutile phase in Fig. 2 (b) also slightly shifted to higher wavelength and its intensity also decreases which might be caused by nanoparticles that covers the nanorods (Balachandran and Eror, 1982; Aprile, *et.al.*, 2008; Luo, *et.al.*, 2014; Ahmad, *et.al.*, 2016).

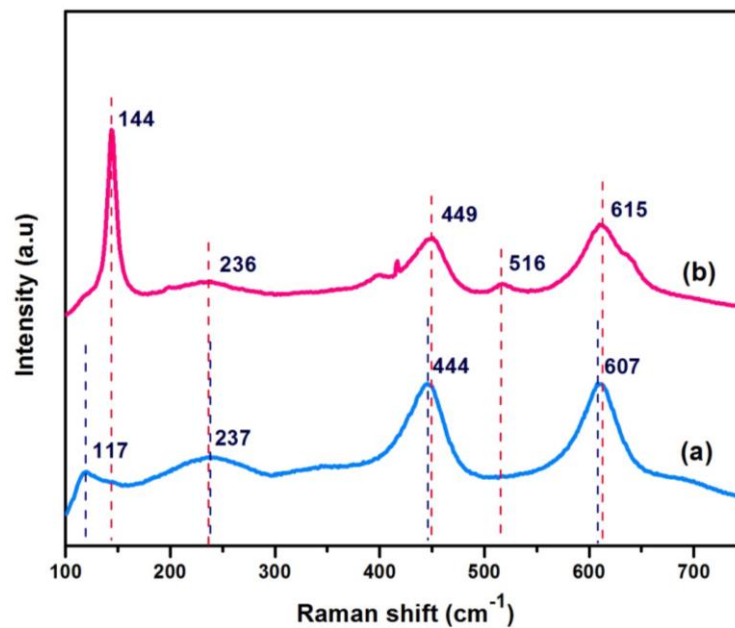


Fig. 2. Micro-Raman spectra of; (a) TiO<sub>2</sub> nanorods and (b) mixed-phase TiO<sub>2</sub> nanostructures.

The  $E_g$  value of fabricated TiO<sub>2</sub> nanostructures were calculated from UV-Vis data. The plotted graph shown

in Fig. 3 shows the large difference of  $E_g$  value between rutile TiO<sub>2</sub> nanorods and mixed-phase TiO<sub>2</sub> nanostructures.

The calculated  $E_g$  for rutile  $\text{TiO}_2$  nanorods is 3.06 eV while the mixed-phase  $\text{TiO}_2$  is 2.84 eV which is in the range of  $\text{TiO}_2$  band gap. The obtained

$E_g$  value of pure rutile is similar with previous report (Lei, *et.al.*, 2016).

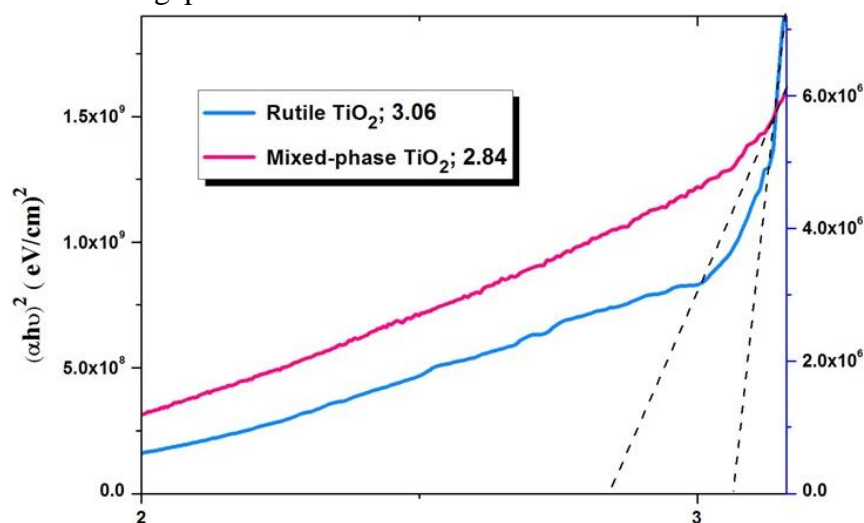


Fig. 3. Band gap value of  $\text{TiO}_2$  nanorods and mixed-phase  $\text{TiO}_2$  nanostructures.

## CONCLUSION

In this study, we successfully synthesized mixed-phase  $\text{TiO}_2$  nanostructures which contains bilayer  $\text{TiO}_2$  nanorods-nanoflowers and nanoparticles. The rutile nanorods-nanoflowers and anatase nanoparticles were synthesized using hydrothermal growth and squeegee method, respectively. The average length of as-grown nanorods were 3.5 nm with the diameter range of 46-215 nm. Meanwhile, the average total thickness and band gap value of mixed-phase  $\text{TiO}_2$  nanostructures were 15.98-24.54 nm and 2.84 eV, respectively. This value is acceptable and the synthesized film has great potential to be applied as photoanode semiconductor layer for DSSCs application.

## ACKNOWLEDGEMENT

The authors would like to express their appreciation to the TWAS-COMSTECH Research Grants (2017-0001-102-11), National Nanotechnology Directorate Division (2014-0015-102-03) and Fundamental Research Grant Scheme (2015-0154-102-02) for financial support on this project.

## REFERENCES

- Ahmad, M. K., S. M. Mokhtar, C. F. Soon, N. Nafarizal, A. B. Suriani, A. Mohamed, M. H. Mamat, M. F. Malek, M. Shimomura, and K. Murakami. 2016. *Raman Investigation of Rutile-phased  $\text{TiO}_2$  Nanorods/Nanoflowers with Various Reaction Times Using One Step Hydrothermal Method*. J. Mater. Sci.: Mater Electron. doi 10.1007/s10854-016-4783-z.

- Ahmad, M. K., V. M. Mohan, and K. Murakami. 2015. *Hydrothermal Growth of Bilayered Rutile-phased TiO<sub>2</sub> Nanorods/Micro-size TiO<sub>2</sub> Flower in Highly Acidic Solution for Dye-sensitized Solar Cell*. J. Sol-Gel Sci. and Technol.73:655-659.
- Aprile, C., L. Maretti, M. Alvaro, J. C. Scaiano, and H. Garcia. 2008. *Long-Lived (Minutes) Photoinduced Charge Separation in A Structured Periodic Mesoporous Titania Containing 2,4,6-triphenylpyrylium as Guest*. Dalton Transactions.5465-5470.
- Balachandran, U. and N. G. Eror. 1982. *Raman Spectra of Titanium Dioxide*. Journal of Solid State Chemistry.42:276-282.
- Bauer, C., G. Boschloo, E. Mukhtar, and A. Hagfeldt. 2002. *Ultrafast Studies of Electron Injection in Ru Dye Sensitized SnO<sub>2</sub> Nanocrystalline Thin Film*. International Journal of Photoenergy.4(1):17-20.
- Diebold, U. 2003. *The Surface Science of Titanium Dioxide*. Surface Science Reports.48:53-229.
- Fukai, Y., Y. Kondo, S. Mori, and E. Suzuki. 2007. *Highly Efficient Dye-sensitized SnO<sub>2</sub> Solar Cells Having Sufficient Electron Diffusion Length*. Electrochemistry Communications.9(7):1439-1443.
- Gong, J., J. Liang, and K. Sumathy. 2012. *Review on Dye-sensitized Solar Cells (DSSCs): Fundamental Concepts and Novel Materials*. Renewable and Sustainable Energy Reviews.16:5848-5860.
- Han, D.-W., J.-H. Heo, D.-J. Kwak, C.-H. Han, and Y.-M. Sung. 2009. *Texture, Morphology and Photovoltaic Characteristics of Nanoporous F:SnO<sub>2</sub> Films*. Journal of Electrical Engineering and Technology.4(1):93-97.
- Hwang, Y. J., C. Hahn, B. Liu, and P. Yang. 2012. *Photoelectrochemical Properties of TiO<sub>2</sub> Nanowire Arrays: A Study of the Dependence on Length and Atomic Layer Deposition Coating*. American Chemical Society.6(6):5060-5069.
- Lee, K.-M., L.-C. Lin, V. Suryanarayanan, and C.-G. Wu. 2014. *Titanium Dioxide Coated on Titanium/Stainless Steel Foil as Photoanode for High Efficiency Flexible Dye-sensitized Solar Cells*. Journal of Power Sources.269:789-794.
- Lei, J., H. Li, J. Zhang, and M. Anpo. 2016. *Mixed-Phase TiO<sub>2</sub> Nanomaterials as Efficient Photocatalysts*. Springer. 423-429.
- Luo, Z., A. S. Poyraz, C.-H. Kuo, R. Miao, Y. Meng, S.-Y. Chen, T. Jiang, C. Wenos, and S. L. Suib. 2014. *Crystalline Mixed Phase (Anatase/Rutile) Mesoporous Titanium Dioxides for Visible Light Photocatalytic Activity*. Chemistry of Materials. dx.doi.org/10.1021/cm5035112.
- Mehmood, U., A. Rahman, K. Harrabi, I. A. Hussein, and B. V. S. Reddy. 2014. *Recent Advances in Dye Sensitized Solar Cells*. Advances in Materials Science and Engineering. <http://dx.doi.org/10.1155/2014/97478>
- O'Regan, B. and M. Grätzel. 1991. *A Low-cost, High-efficiency Solar Cell Based on Dye-Sensitized Colloidal TiO<sub>2</sub> Films*. Nature. 353:737-740.
- Qin, D.-D., Y.-P. Bi, X.-J. Feng, W. Wang, G. D. Barber, T. Wang, Y.-M. Song, X.-Q. Lu, and T. E. Mallouk. 2015. *Hydrothermal Growth and*

- Photoelectrochemistry of Highly Oriented, Crystalline Anatase TiO<sub>2</sub> Nanorods on Transparent Conducting Electrodes.* Chemistry of Materials.27:4180-4183.
- Sima, C., C. Grigoriu, and S. Antohe. 2010. *Comparison of the Dye-sensitized Solar Cells Performances Based on Transparent Conductive ITO and FTO.* Thin Solid Films.519:595-597.
- Tamilselvan, V., D. Yuvaraj, R. R. Kumar, and K. N. Rao. 2012. *Growth of Rutile TiO<sub>2</sub> Nanorods on TiO<sub>2</sub> Seed Layer Deposited by Electron Beam Evaporation.* Applied Surface Science.258:4283-4287.
- Zhang, D., T. Yoshida, T. Oekermann, K. Furuta, and H. Minoura. 2006. *Room-temperature Synthesis of Porous Nanoparticulate TiO<sub>2</sub> Films for Flexible Dye-sensitized Solar Cells.* Advanced Functional Materials.16:1228-1234.
- Zhu, M., X. Li, W. Liu, and Y. Cui. 2014. *An Investigation on The Photoelectrochemical Properties of Dye-sensitized Solar Cells Based on Graphene- TiO<sub>2</sub> Composite Photoanodes.* Journal of Power Sources.262:349-355.